



A guide to the otoliths of Southern Ocean lanternfishes (Myctophidae)

Darren W. Stevens¹ · Heather E. Braid² · Laureline Meynier³ · Pablo C. Escobar-Flores¹ · Matthew H. Pinkerton¹ · Doug Hopcroft⁴ · Yanyu He⁴ · Yves Cherel⁵

Received: 11 July 2024 / Revised: 20 September 2024 / Accepted: 24 September 2024 / Published online: 22 October 2024
© The Author(s) 2024

Abstract

In the Southern Ocean, myctophids (family Myctophidae) are speciose, dominate the mesopelagic fish biomass, and are important in the diets of many fishes, squids, seabirds, and marine mammals. Consequently, they play a key role in carbon export and energy transfer from primary consumers to top predators. However, they are delicate and rarely found intact in predator stomachs, which makes them difficult to identify to species. Fortunately, their otoliths (sagittae) are mostly distinctive and therefore useful for species identification. Previous studies describing Southern Ocean myctophid otoliths were often limited by small sample sizes or focused on only a few species. To facilitate myctophid identifications in diet studies, we provide scanning electron microscope images of otoliths with brief descriptions for 37 species of Southern Ocean myctophids. The identities of problematic taxa were confirmed with DNA. Most species were found to have distinctive otoliths, which can be used to identify them to the species level. Large *Gymnoscopelus piabilis* otoliths comprised two types, which may represent different species. In addition, allometric equations are provided for 32 species to enable back calculation of fish size.

Keywords Diet · Mesopelagic fish · Allometric equations · Sagittae · Trophic relationships

Introduction

Myctophids or lanternfishes (family Myctophidae) are an abundant and speciose family comprising *c.* 250 species in 34 genera (Fricke et al. 2024) and are found in all oceans at mesopelagic to bathypelagic depths.

In the Southern Ocean (SO; water masses south of the Subtropical Front), myctophids are the dominant mesopelagic fish, with a biomass estimate of 70–570 million tonnes in Antarctic waters (Lancraft et al. 1989; Sabourenkov 1992; Dornan et al. 2022). There are over 30 SO myctophid species, and they range in maximum size from *c.* 54 mm fish standard length, L_S , (*e.g.*, *Protomyctophum tenisoni*) to *c.* 280 mm L_S (*Gymnoscopelus bolini*; Hulley 1981). Most species are high-oceanic (except for *Lampanyctodes hectoris*, which is pseudoceanic) and mesopelagic (Hulley 1981)—although some *Gymnoscopelus* species appear to be benthopelagic at times (Saunders et al. 2021)—but they vary significantly in their vertical and areal distribution (see distributional patterns of Hulley 1981, Table 3).

Myctophids facilitate the export of organic carbon through diel vertical migration, feeding during the night higher in the water column and excreting and respiring in deeper water during the day (Davison et al. 2013). They are

Deceased: Doug Hopcroft.

✉ Darren W. Stevens
Darren.Stevens@niwa.co.nz

¹ National Institute of Water and Atmospheric Research Limited (NIWA), P.O. Box 14-901, Kilbirnie, Wellington 6021, New Zealand

² AUT Lab for Cephalopod Ecology & Systematics (ALCES), School of Science, Auckland University of Technology, Private Bag 92006, Auckland 1142, New Zealand

³ Bioresearches Group, Babbage Consultants Limited, Level 4, 68 Beach Road Shortland Street, PO Box 2027, Auckland 1140, New Zealand

⁴ Manawatu Microscopy and Imaging Centre, Massey University, Private Bag 11 222, Palmerston North 4410, New Zealand

⁵ Centre d'Etudes Biologiques de Chizé, UMR 7372 du CNRS-La Rochelle Université, 79360 Villiers-en-Bois, France

a crucial component of SO food webs (Saunders et al. 2021), feeding primarily on planktonic crustaceans (Saunders et al. 2019), and playing a key role in the transfer of energy from primary consumers (zooplankton) to top predators (Cherel et al. 2010; Saunders et al. 2019), including penguins (Brown and Klages 1987; Cherel et al. 2002), petrels (Connan et al. 2007), seals (Cherel et al. 1997; Reisinger et al. 2018), squids (Phillips et al. 2001), and fishes (Goldsworthy et al. 2001; Collins et al. 2007).

The accurate identification of SO myctophid prey is critical to understanding predator trophodynamics (Saunders et al. 2021). However, myctophid identification is often based on characters that are lost during ingestion and digestion (for example, the number and arrangement of luminescent photophores). Fortunately, myctophid sagittal otoliths (hereafter otoliths) have useful taxonomic characters that can be used for species identification. However, the otoliths of some species are remarkably similar (for example *Gymnoscopelus fraseri* and *G. hintonoides*), particularly when eroded.

Several previous studies have provided diagnostic criteria for otoliths and otolith:fish size regressions for SO myctophids (e.g., Schwarzahns (1984); Hecht 1987; Williams and McEldowney 1990; Smale et al. 1995; Reid 1996; Furlani et al. 2007; Schwarzahns 2019). However, the sample sizes in these studies were often small and limited to relatively few species.

Based on published literature (Hulley 1981; Duhamel et al. 2005; Roberts et al. 2015) and trophic data from the Crozet and Kerguelen Islands, we recognise 37 species of

SO myctophids and provide representative SEM (scanning electron microscopy) otolith images and diagnostic criteria for these species. We also provide otolith length (O_L): L_S and fish mass (M_T): L_S regressions for 32 species (there were too few otoliths to provide regressions for the remaining five SO species) to enable back calculation of prey size.

Materials and methods

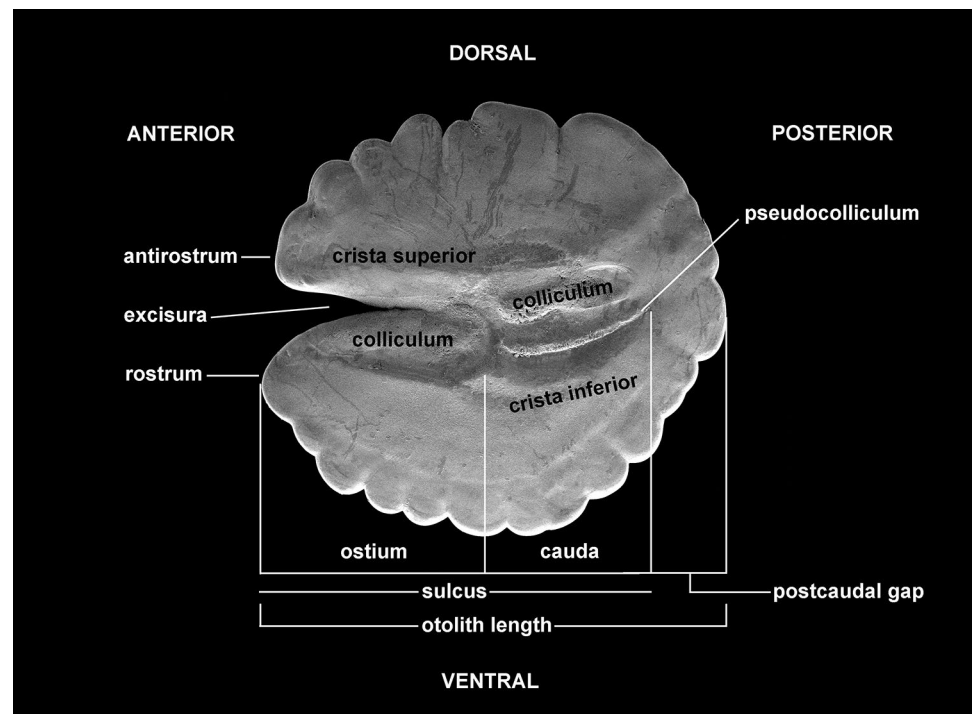
Samples

Myctophids were collected opportunistically from research surveys around Aotearoa New Zealand (mainly Chatham Rise and sub-Antarctic waters over the Campbell Plateau), the outer Ross Sea, and off the Kerguelen and South Shetland Islands. Myctophids were identified using the following publications: Hulley (1981); Smith and Heemstra (2003); and Roberts et al. (2015). Where possible, each fish was measured (L_S to the nearest mm), weighed (M_T to the nearest gram), and sexed, and their otoliths extracted.

Each otolith was placed in water in a petri dish, cleaned of endolymphatic sac remnants, dried on blotting paper, placed in a labelled Eppendorf® tube, and stored dry in a labelled paper envelope.

Otolith terminology largely follows Smale et al. (1995) (Fig. 1). However, the term “excisura” (i.e., excisural notch, Smale et al. 1995) is used to refer to the anterior incision into the ostium between the antirostrum and the rostrum, as per the original meaning in Koken 1884 (W.

Fig. 1 Scanning electron microscopy image of the mesial (inner) surface of a right sagitta of *Metelectrona ventralis* labelled with the terminology used in this study (after Smale et al. 1995)



Schwarzahns, personal communication). The term “ostial furrow” (Schwarzahns 1981 (1984)) is also used to refer to the grooved indentation that runs from the excisura through the ostium, and the term “denticles” (Schwarzahns 2013) is used for the projections on the ventral margin of the otoliths of some myctophid species. Denticles can be further subdivided by shape, e.g., crenate (rounded scalloped projections), serrate (regular sawtooth-like projections), and sinuate (regular wave-like curved projections) (Smale et al. 1995). Where possible, the mesial (inner) surface of the right otolith was measured with a calibrated dissecting microscope. O_L was measured from the greatest distance between the rostrum and posterior margin, excluding any posteriorly directed ventral serrations (e.g., some *Diaphus* species or *Lampanyctodes hectoris* otoliths), and as measured with the sulcus in the horizontal plane (Fig. 1). Generally, O_L was measured from the rostrum to the posterior margin adjacent to the sulcus, while in other cases (e.g., some *Protomyctophum* species), the O_L was measured from the rostrum to the flared posterodorsal extension.

Scanning electron microscopy (SEM)

Otoliths were mounted onto numbered SEM specimen stubs with double-sided cellulose tape. Mounted otoliths were sputter-coated with a thin layer of gold for 200 s. Otolith micrographs were taken at the Manawatū Microscopy and Imaging Centre using a FEI Quanta 200 SEM at an accelerating voltage of 20.0 kV following standard protocols.

Digital SEM otolith images were edited and compiled in Adobe® Photoshop®. Each otolith image was rotated so that the sulcus was in the horizontal plane, adjusted for brightness and contrast, a black background fill layer was added, and a scale bar inserted. Otolith images with small amounts of extraneous matter were digitally altered to remove the matter. Otolith images with larger amounts of extraneous matter (usually remaining adhesive when an otolith was imaged on both sides) were not used or the otoliths were cleaned by briefly placing in a shallow bath of acetone, and then re-imaged.

DNA barcoding

DNA from taxonomically challenging *Protomyctophum* species was extracted from dorsal muscle tissue using EconoSpin columns (Epoch Life Science) with QIAGEN reagents following protocols for the DNeasy Blood and Tissue Kit (QIAGEN). The DNA barcode region—648bp from the 5' end of the mitochondrial gene cytochrome *c* oxidase subunit I (COI)—was amplified using the primer pair LCO1490/HCO2198 (Folmer et al. 1994) or C_VF1LFt1/C_VR1LRt1 (Ivanova et al. 2007) following protocols from Braid et al. (2014). PCR products showing a single, clear band on 1%

agarose gels stained with GelRed (Biotium) were bi-directionally sequenced by Macrogen (Korea) using the same primers used for PCR (for LCO1490/HCO2198) or with universal M13 sequencing primers M13-FP/M13R-pUC (for C_VF1LFt1/C_VR1LRt1). Bi-directional sequences were concatenated and edited in CodonCode Aligner (CodonCode Corp., Dedham, MA, USA). Sequences were uploaded to the Barcode of Life Data System (Ratnasingham and Hebert 2007) public project titled ‘Lanternfish from Aotearoa’ (project code: LAN) and subsequently submitted to GenBank. All sequences were screened for potential contamination using GenBank’s Basic Local Alignment Search Tool (BLAST).

Myctophid identifications were confirmed using the Barcode Index Number (BIN) analysis in BOLD that uses a clustering algorithm to automatically generate operational taxonomic units based on COI, which have a high concordance with species (Ratnasingham and Hebert 2013).

Results

Myctophid otoliths come in a variety of shapes, but they are generally approximately oval-ovate, discoid, or kidney-shaped. In addition, they are united by the presence of a shallow horizontal sulcus and a pseudo-colliculum (a small ridge under the cauda) (Smale et al. 1995). Most SO myctophids were identifiable by their otoliths. The number of otoliths examined for each species and regressions for O_L to fish size (to enable prey size to be estimated) where sufficient otoliths were available are provided in the Appendix. To enable comparison between species, the estimated O_L and M_T of a 50 mm L_S fish are provided for species with regression data in the Appendix.

Otolith (sagitta) identification

Key diagnostic otolith characters are provided for the 37 SO species. For ease of use, the otolith characters for each species follow the order used for the otolith SEM images in Figs. 2, 3, 4, 5 and 6. More comprehensive otolith descriptions can be found in other references, for example Smale et al. (1995), Schwarzahns (2013, 2019). The maximum known otolith length, O_{Lmax} , is provided for each species.

Diaphus danae (6.0 mm O_{Lmax}), *D. hudsoni* (5.7 mm O_{Lmax} ; Smale et al. 1995), and *D. ostenfeldi* (6.0 mm O_{Lmax}) have rounded-ovate otoliths with serrate ventral margins (Fig. 2; Schwarzahns 2013). *Diaphus danae* otoliths (Fig. 2) have a rostrum that is much longer than the antirostrum and the dorsal margin is raised posteriorly to form a papilla (Furlani et al. 2007). In contrast, *Diaphus ostenfeldi* otoliths (Fig. 2) have a shorter rostrum and a dorsal margin that is raised anteriorly and depressed

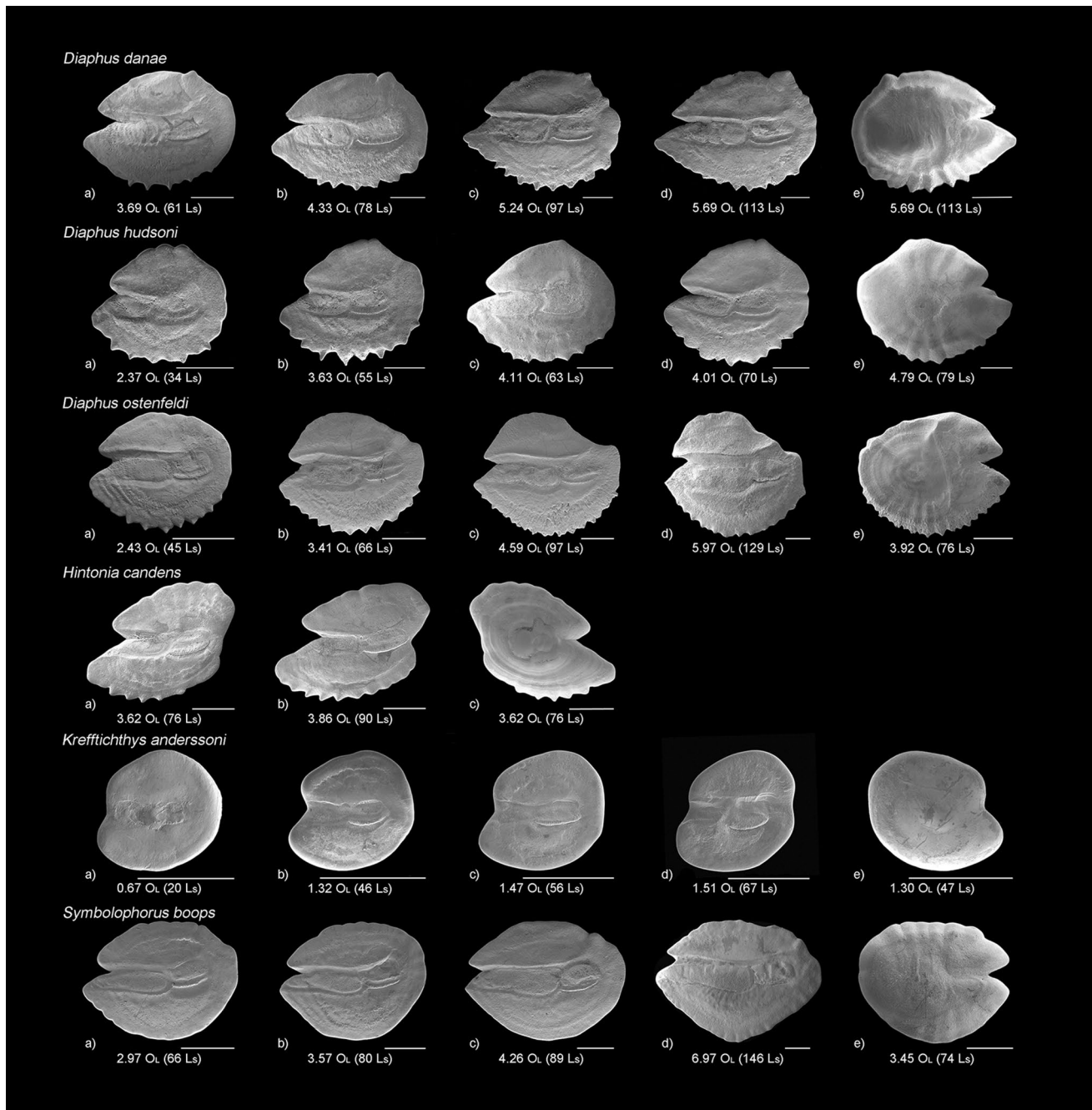


Fig. 2 Scanning electron microscopy images of the mesial (generally **a–d**) and lateral (last image) surface of selected otoliths (sagittae) of *Diaphus danae*, *D. hudsoni*, *D. ostensfeldi*, *Hintonia candens*, *Kref-*

fichthys anderssoni, and *Symbolophorus boops*. O_L , otolith length in mm, L_S , fish standard length in mm. *S. boops* otolith image **d** has been flipped horizontally. Scale bar represents 1 mm

(notched) posteriorly (Smale et al. 1995; Schwarzahns 2013). The otoliths of *D. hudsoni* (Fig. 2) are more compact with more rounded rostra, a cauda and ostium of similar size (*versus* a larger ostium, Schwarzahns 2013), and a longer postcaudal gap. These three species also differ in the number of ventral denticles, with *D. ostensfeldi* having more denticles (12–13) than *D. hudsoni* (9–11) or *D. danae* (8–10, Schwarzahns 2013). Small *Diaphus* otoliths

(< c. 3 mm O_L) often lack key diagnostic characters and may not be identifiable to the species level (Schwarzahns 2013).

Hintonia candens (only two otolith pairs examined, largest 4.0 mm O_L) otoliths (Fig. 2) are oblong-ovate with prominent rostra, a moderate excisura, a dorsal margin that is raised and extended posteriorly, and a serrate ventral margin.

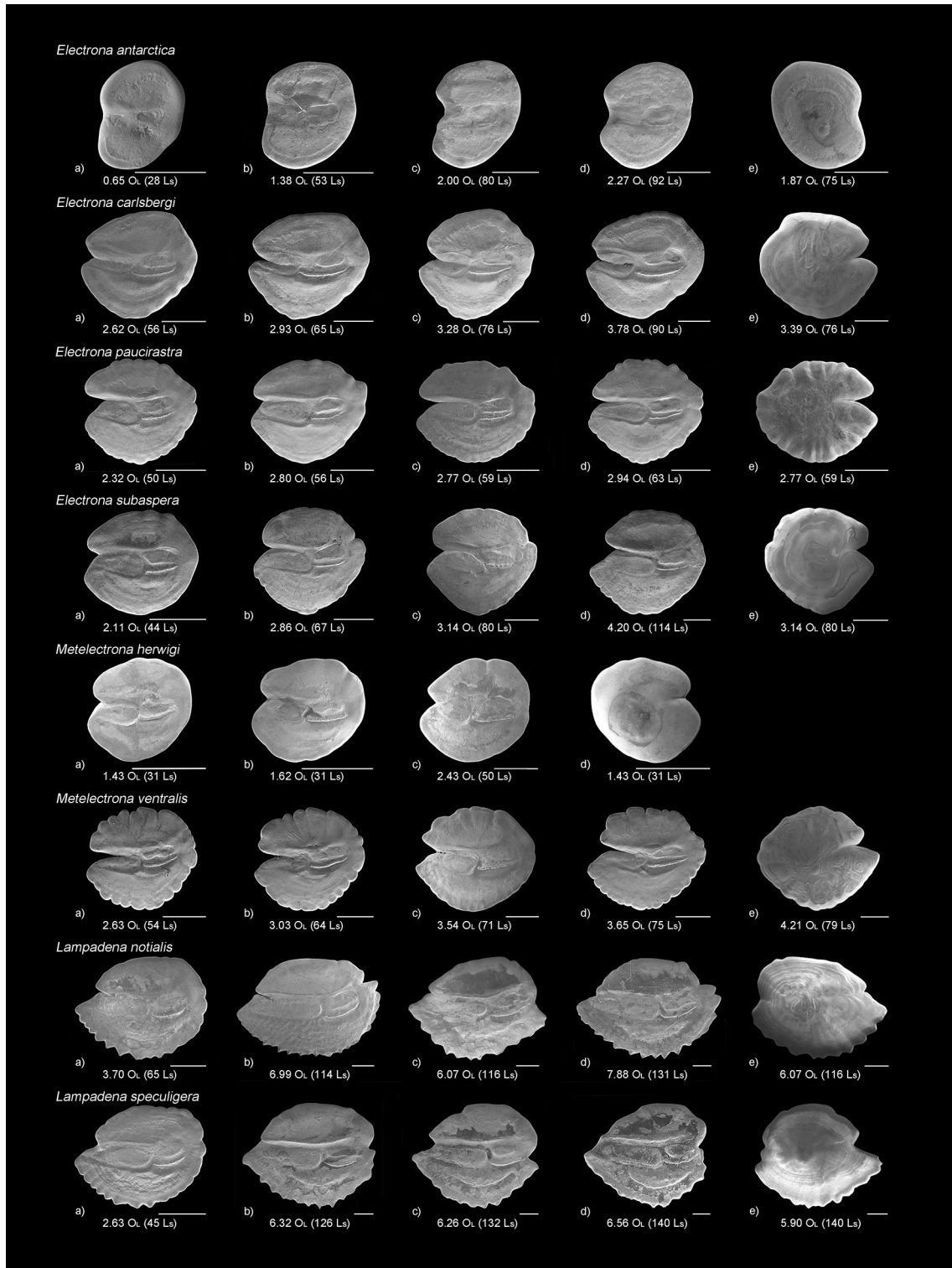


Fig. 3 Scanning electron microscopy images of the mesial (generally a–d) and lateral (last image) surface of selected otoliths (sagittae) of *Electrona antarctica*, *E. carlsbergi*, *E. paucirastra*, *E. subaspera*,

Metelectrona herwigi, *M. ventralis*, *Lampadena notialis*, and *L. speculigera*. O_L, otolith length in mm, L_S, fish standard length in mm. Scale bar represents 1 mm

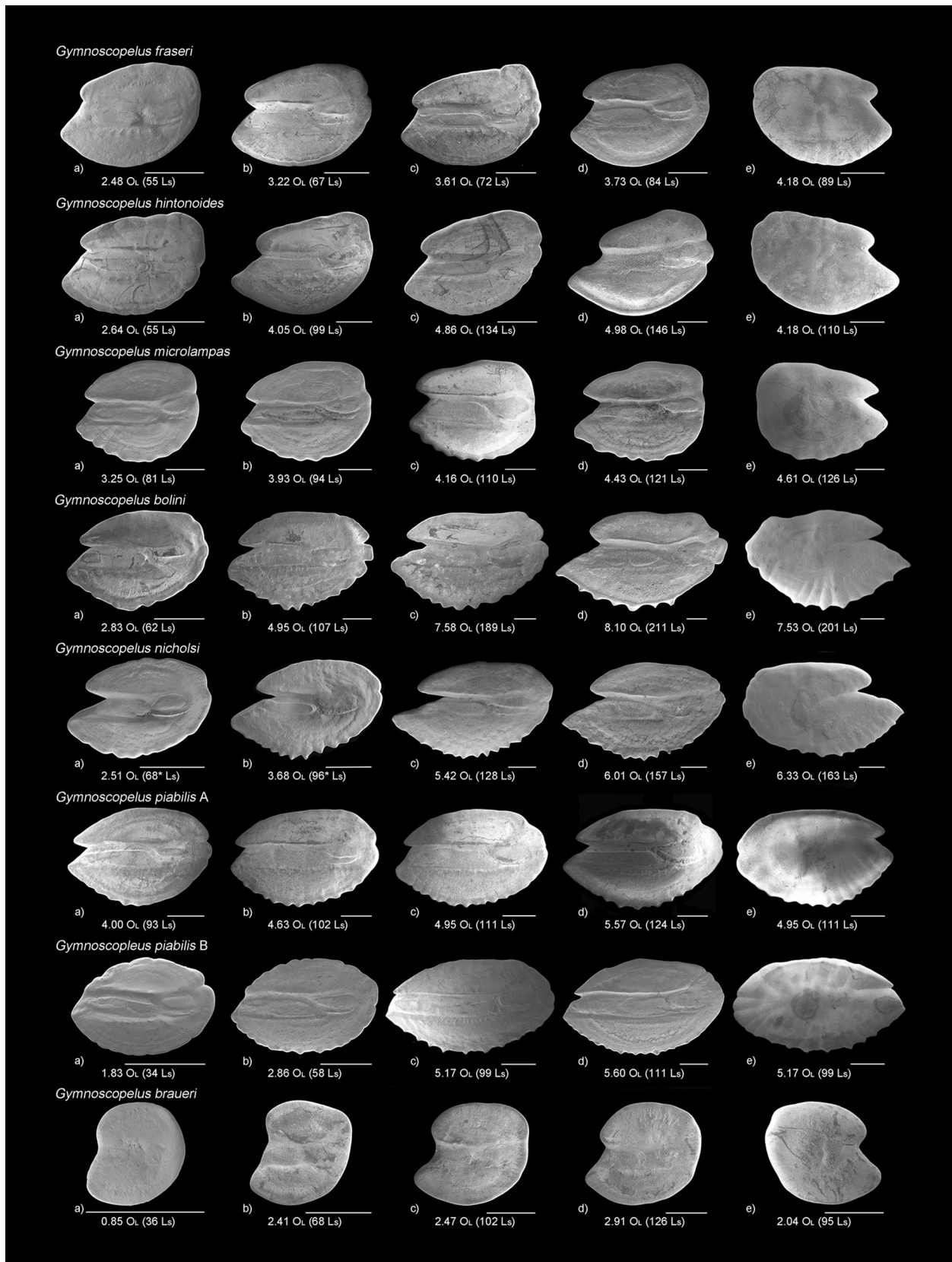


Fig. 4 Scanning electron microscopy images of the mesial (a–d) and lateral (e) surface of selected otoliths (sagittae) of *Gymnoscopelus fraseri*, *G. hintonoides*, *G. microlampas*, *G. bolini*, *G. nicholsi*, *G. piabilis* A, *G. piabilis* B, and *G. braueri*. O_L , otolith length in mm, L_S , fish standard length in mm. *, L_S estimated based on $L_S:O_L$ regression (Appendix). *G. nicholsi* otolith image a and *G. piabilis* B otolith image a have been flipped horizontally. Scale bar represents 1 mm

Krefflichthys anderssoni (1.9 mm O_{Lmax} ; Smale et al. 1995) otoliths (Fig. 2) are discoid to kidney shaped with short very broad rostra and depressed colliculi (Smale et al. 1995).

Symbolophorus boops (7.0 mm O_{Lmax}) otoliths are oval to oblong-ovate with slightly crenate to irregular margins (Smale et al. 1995; Fig. 2).

Electrona antarctica (2.6 mm O_{Lmax}) otoliths (Fig. 3) are tall (high), and comma/kidney shaped (reniform) with short poorly developed rostra and a short slightly raised pseudocolliculum (Williams and McEldowney 1990; Smale et al. 1995). They have the most distinctive otoliths in the genus (Fig. 3) but can be confused with those from *Protomyctophum bolini* and small otoliths of *Gymnoscopelus braueri* (see below). *Electrona carlsbergi* (4.5 mm O_{Lmax}), *E. paucirastra* (3.4 mm O_{Lmax}), and *E. subaspera* (4.3 mm O_{Lmax}) have similar high relief discoid otoliths (Williams and McEldowney 1990; Fig. 3). *Electrona carlsbergi* otoliths (Fig. 3) have an antirostrum that is almost as wide as the rostrum, a central ostial furrow, and a pseudocolliculum that is longer than the posterior colliculum (Smale et al. 1995; Reid 1996). Note that the otolith of “*E. carlsbergi*” in Fig. 4 of Rodhouse et al. (1992) refers to *P. choriodon*. *Electrona paucirastra* and *E. subaspera* otoliths (Fig. 3) have an antirostrum that is usually significantly smaller than the rostrum, an ostial furrow that is approximately level with the crista superior (Reid 1996), a pseudocolliculum that is about the same length as the posterior colliculum, and large otoliths may have a posterior bulge, an extension of the ventral margin (Williams and McEldowney 1990). Although the otoliths of these two species are similar, *Electrona paucirastra* is a smaller species (to 70 mm vs. 127 mm L_S in *E. subaspera*; Smith and Heemstra 2003) with smaller but broader otoliths, and a generally narrower antirostrum.

Metelectrona herwigi (2.4 mm O_{Lmax}) and *M. ventralis* (4.5 mm O_{Lmax}) have discoid otoliths (Fig. 3) that are similar to those of *Electrona* species, a rostrum that is larger than the antirostrum, an ostial furrow that is approximately level with the crista superior, and a pseudocolliculum that is longer than the posterior colliculum. *Metelectrona ventralis* otoliths often have crenate to cockscomb-like margins (otoliths < 2.2 mm O_L have not been examined), while those of *M. herwigi* are entire. *Metelectrona herwigi* is a smaller species (to 59 mm L_S versus 107 mm L_S in *M. ventralis*;

Hulley 1981) so otoliths larger than c. 3.0 mm O_L are likely to be *M. ventralis*.

Lampadena notialis (9.3 mm O_{Lmax}) and *L. speculigera* (7.8 mm O_{Lmax}) otoliths (Fig. 3) are oval-ovate, variable, and difficult to separate, although large *L. speculigera* otoliths may appear truncated posteriorly (triangular-ovate), and the pseudocolliculum is often more strongly curved anteriorly, terminating well above the ventral margin of the ostium versus approximately level with it in *L. notialis*.

Gymnoscopelus fraseri (4.2 mm O_{Lmax}) and *G. hintonoides* (5.1 mm O_{Lmax}) otoliths (Fig. 4) are oblong-ovate with a raised, right-angled but rounded, postero-dorsal margin (Smale et al. 1995; this study). Otoliths of both species are remarkably similar and difficult to separate but *G. hintonoides* otoliths generally have larger more prominent rostra, the dorsal margin is more strongly raised posteriorly, and large otoliths may have a postcaudal lobe. References to *G. “hintonoides”* otoliths in Williams and McEldowney (1990) appear to be those of *G. opisthopterus*. *Gymnoscopelus microlampas* (4.7 mm O_{Lmax}) otoliths (Fig. 4) are similar to those of *G. fraseri* and *G. hintonoides* but they are more compact with similar length rostra, an almost straight posterior margin, and a weakly crenulated ventral margin (Williams and McEldowney 1990; Fig. 4).

Gymnoscopelus bolini (9.5 mm O_{Lmax}) and *G. nicholsi* (6.6 mm O_{Lmax}) otoliths (Fig. 4) are oblong-ovate to elongate with a short (*G. bolini*) to moderate (*G. nicholsi*) sharply rounded antirostrum, a large broad sharply pointed to rounded rostrum, and a serrated ventral margin (Smale et al. 1995). Large *G. bolini* and *G. nicholsi* otoliths are similar; however, *G. bolini* grows much larger (to 280 vs 161 mm L_S for *G. nicholsi*; Hulley 1981) and has larger otoliths, so at a given otolith length, *G. nicholsi* otoliths have more prominent sharply pointed rostra than those of *G. bolini* (Fig. 4; see otolith illustrations of a 56 mm L_S *G. bolini* and a 55 mm L_S *G. nicholsi* in Williams and McEldowney 1990), and otoliths longer than c. 6.8 mm O_L are likely to be *G. bolini*. *Gymnoscopelus piabilis* (6.3 mm O_{Lmax}) otoliths (Fig. 4) are oblong to oblong-ovate with a serrate ventral margin (Smale et al. 1995). The otoliths are variable and may comprise two species (McBride et al. 2022). Larger otoliths fall into two types: a more compact form with larger rostra and a larger excisura (*Gymnoscopelus piabilis* A, Fig. 4; Williams and McEldowney 1990, Fig. 18), and a more elongate form with small rostra and a slight excisura (*Gymnoscopelus piabilis* B, Fig. 4; Smale et al. 1995, Plate 20 F2–F4). Otoliths of *G. piabilis* A are similar to those of *G. nicholsi* and *G. bolini*, but the rostrum is generally shorter, and the ventral margin is often less serrate.

Gymnoscopelus braueri (3.0 mm O_{Lmax} ; Smale et al. 1995) otoliths (Fig. 4) are approximately ovate with rounded rostra while *G. opisthopterus* (3.5 mm O_{Lmax}) otoliths

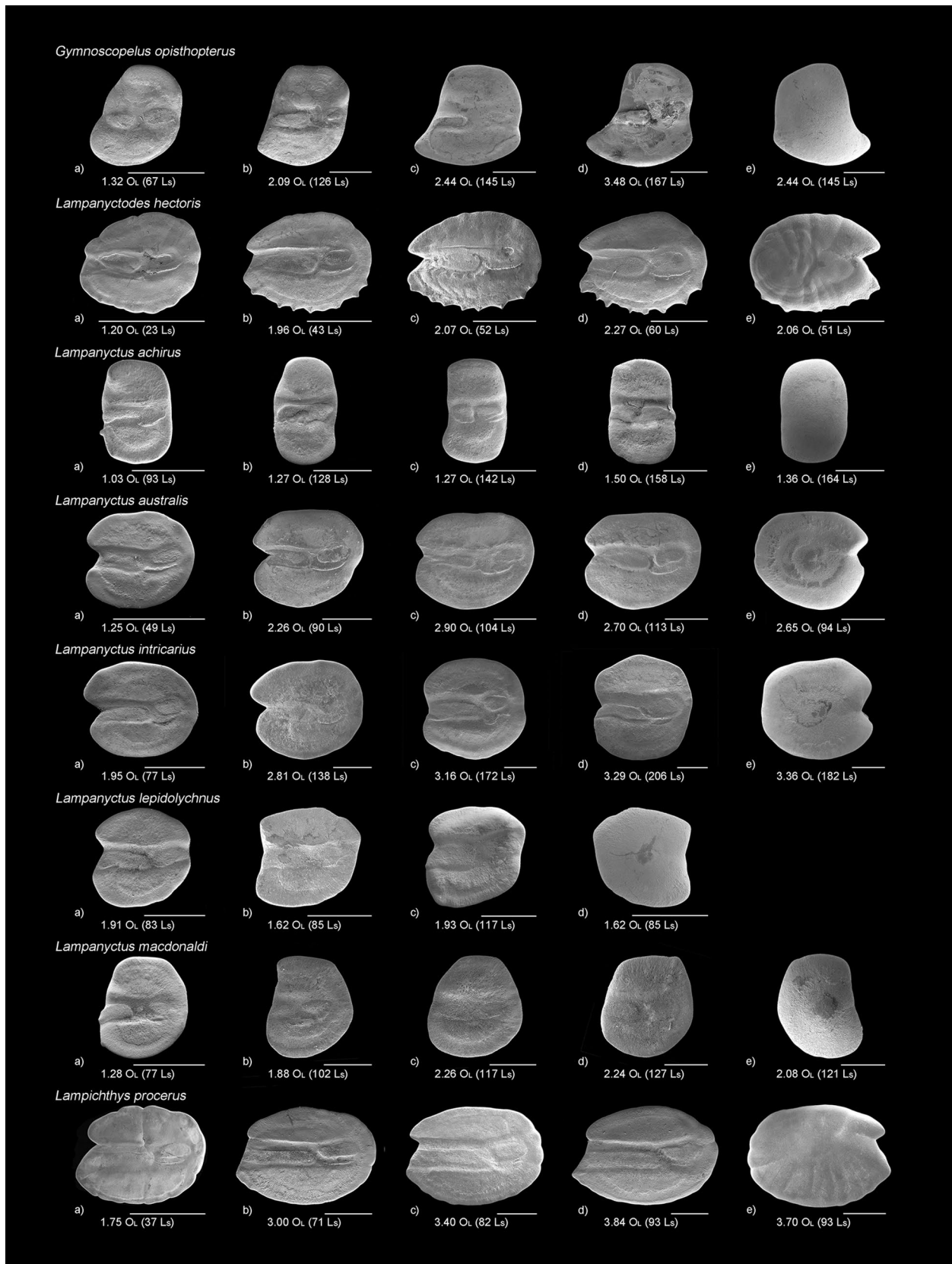


Fig. 5 Scanning electron microscopy images of the mesial (generally a–d) and lateral (last image) surface of selected otoliths (sagittae) of *Gymnoscopelus opisthopterus*, *Lampanyctodes hectoris*, *Lampanyctus achirus*, *L. australis*, *L. intricarius*, *L. lepidolychnus*, *L. macdonaldi*, and *Lampichthys procerus*. O_L , otolith length in mm, L_S , fish standard length in mm. *L. australis* otolith image **a** and *L. intricarius* otolith images **a** and **d** images have been flipped horizontally. Scale bar represents 1 mm

(Fig. 5) are tall and ear shaped, generally with no antirostrum (or a very slight antirostrum), and a slight to prominent sharply pointed rostrum in large otoliths (Smale et al. 1995; this study). The otoliths of small fish (to c. 70 mm L_S) of both species are similar, although, *G. braueri* otoliths have a shallower sulcus.

Lampanyctodes hectoris (2.7 mm O_{Lmax}) otoliths are rounded-ovate to oval-ovate with a sinuate to serrate ventral margin (Smale et al. 1995; Fig. 5).

Lampanyctus achirus (1.6 mm O_{Lmax}) (previously assigned to *Nannobranchium*, which has since been synonymised; Martin et al. 2018) has tall, rectangular otoliths with no rostra, and approximately parallel anterior and posterior margins (Smale et al. 1995; Fig. 5). *Lampanyctus australis* (3.1 mm O_{Lmax}) and *L. intricarius* (3.8 mm O_{Lmax}) have similar otoliths (Fig. 5); in small specimens, the otoliths of both species are oval-obovate, but in larger *L. intricarius*, the otoliths are discoid. *Lampanyctus intricarius* grows significantly larger than *L. australis* (to 212 mm versus 131 mm L_S ; Hulley 1981; this study) so discoid otoliths and/or those longer than c. 3.1 mm are likely to be *L. intricarius*. In addition, *L. australis* otoliths generally have a flattened dorsal margin. *Lampanyctus lepidolychnus* (2.4 mm O_{Lmax} ; Smale et al. 1995) otoliths are tall, and approximately kidney shaped with short rostra and a very slight or no postcaudal gap versus a short to moderate postcaudal gap in *L. australis*, *L. intricarius*, and *L. macdonaldi* (Smale et al. 1995; this study, Fig. 5). *Lampanyctus macdonaldi* (2.6 mm O_{Lmax}) otoliths are variable, approximately ear shaped to somewhat discoid, generally lack an antirostrum and have a very short and broad rostrum (Smale et al. 1995; Fig. 5).

Lampichthys procerus (4.1 mm O_{Lmax}) has oval-ovate otoliths with a short narrow sharply rounded antirostrum, a short, broad rostrum that can be angled, pointed, or sharply rounded, and an entire (or slightly irregular) ventral margin (Smale et al. 1995; Fig. 5).

Protomyctophum otoliths are approximately kidney shaped, the dorsal and ventral margins are often slightly bulbous, the ostium and cauda are more or less equal in length, the pseudo-colliculum is long, ridge-like and projects anteriorly beyond the posterior colliculum, and the excisura is wide (Schwarzhan 1981 (1984); Smale et al. 1995; Fig. 6). Larger otoliths are generally broader dorsally and more strongly keeled/undercut ventrally. The otoliths of many species are similar and identification beyond genus is

often difficult, particularly with eroded otoliths. *Protomyctophum choriodon* (2.5 mm O_{Lmax}) and *P. tenisoni* (1.8 mm O_{Lmax} , Smale et al. 1995) are elongate species with significantly smaller otoliths than other *Protomyctophum* species (Figs. 6, 7). Their otoliths are broad with relatively large, rounded rostra, a generally short postcaudal gap, and they are strongly keeled. *Protomyctophum choriodon* otoliths have a prominent excisura, generally an anteroventral indentation, and in some larger otoliths a posteroventral indentation. The otolith of *P. "normani"* in Smale et al. (1995) refers to *P. choriodon* (A. Hulley, personal communication). *Protomyctophum tenisoni* otoliths have more rounded rostra and often have a largely straight posterior margin.

Protomyctophum andriashevi (2.4 mm O_{Lmax}) otoliths are strongly keeled and often have a distinct pit posterior to the colliculum (Fig. 6). *Protomyctophum bolini* (2.1 mm O_{Lmax}) otoliths are narrow, with short, very broad rostra and often have a postcaudal indentation (Reid 1996; Figs. 6, 7); although, otoliths from large specimens from the sub-Antarctic in Aotearoa New Zealand are broader dorsally (possibly indicative of older fish) and more strongly keeled. The otoliths of *P. parallelum* (only one otolith pair examined, 1.85 mm O_{Lmax} , Williams and McEldowney 1990) are similar to those of *P. bolini*, but *P. parallelum* otoliths have larger rostra, are strongly keeled, and have a large postcaudal gap (Fig. 6).

Protomyctophum gemmatum, *P. luciferum*, and *P. normani* comprise the *P. normani*-complex (Hulley 1981). These species (and their otoliths) are similar and are often difficult to identify to species. Problematic specimens of *P. gemmatum* and *P. luciferum* were barcoded to confirm their identity. *Protomyctophum normani* is the smallest species in the complex (to 56 mm L_S ; Hulley 1981) with relatively smaller otoliths (2.3 mm O_{Lmax}) that have a short postcaudal gap (Figs. 6, 7). *Protomyctophum luciferum* and *P. gemmatum* are larger species (to 70 mm & 86 mm L_S respectively, this study; Hulley 1981) with larger otoliths (3.3 mm and 3.9 mm O_{Lmax} , respectively; Figs 6, 7) with a longer postcaudal gap. Large *P. luciferum* otoliths are often flattened and broader dorsally while *P. gemmatum* generally have larger more rounded otoliths, with a more pointed antirostrum, which is often slightly indented dorsally.

Discussion

This study complements previous studies on the identification of SO myctophid otoliths (Schwarzhan 1981 (1984), 2013, 2019; Hecht 1987; Williams and McEldowney 1990; Smale et al. 1995; Reid 1996; Furlani et al. 2007) and provides diagnostic criteria and SEM images for 37 SO species. Our results are consistent with these earlier studies, in that larger intact otoliths of most SO myctophids have

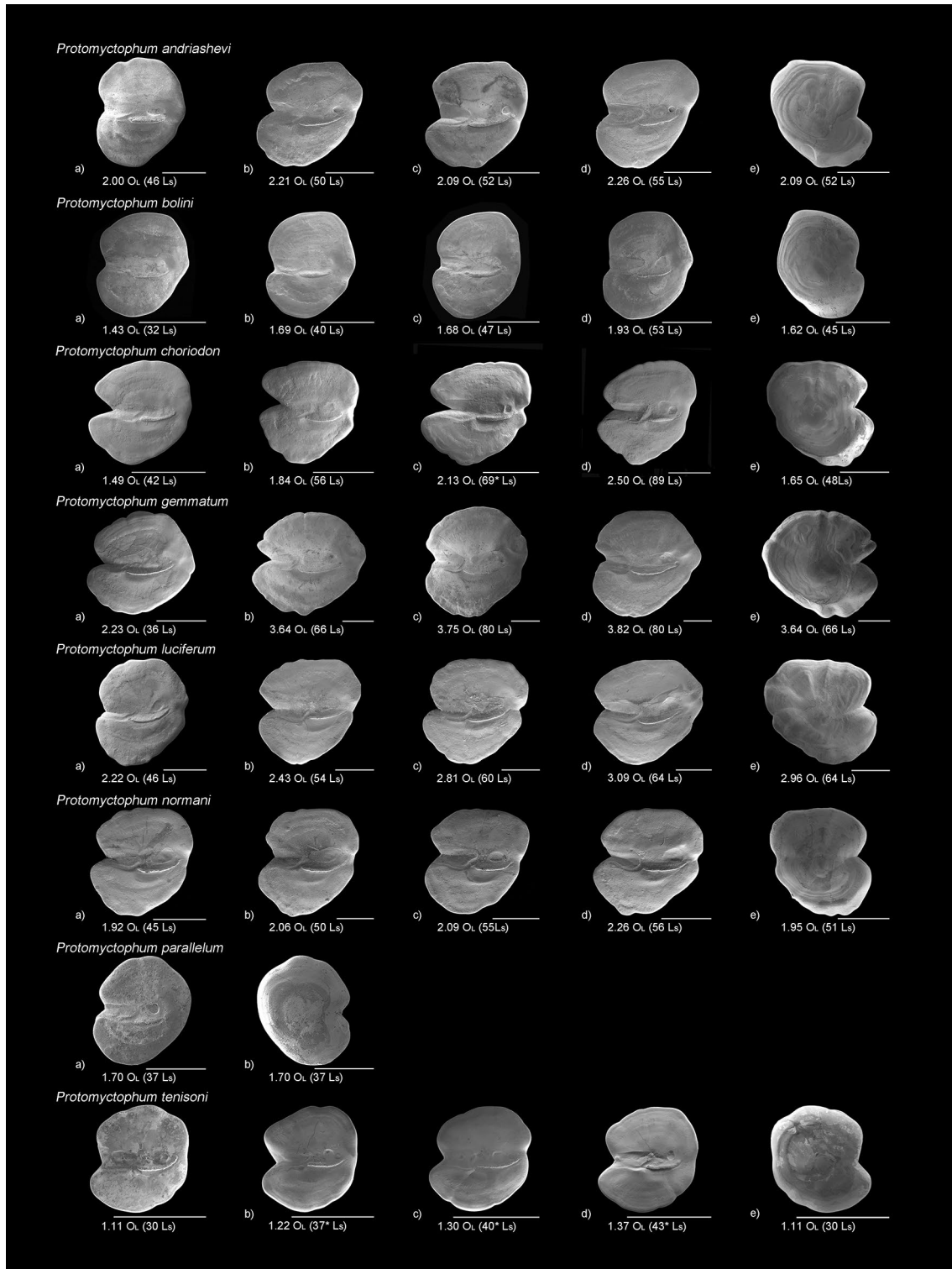
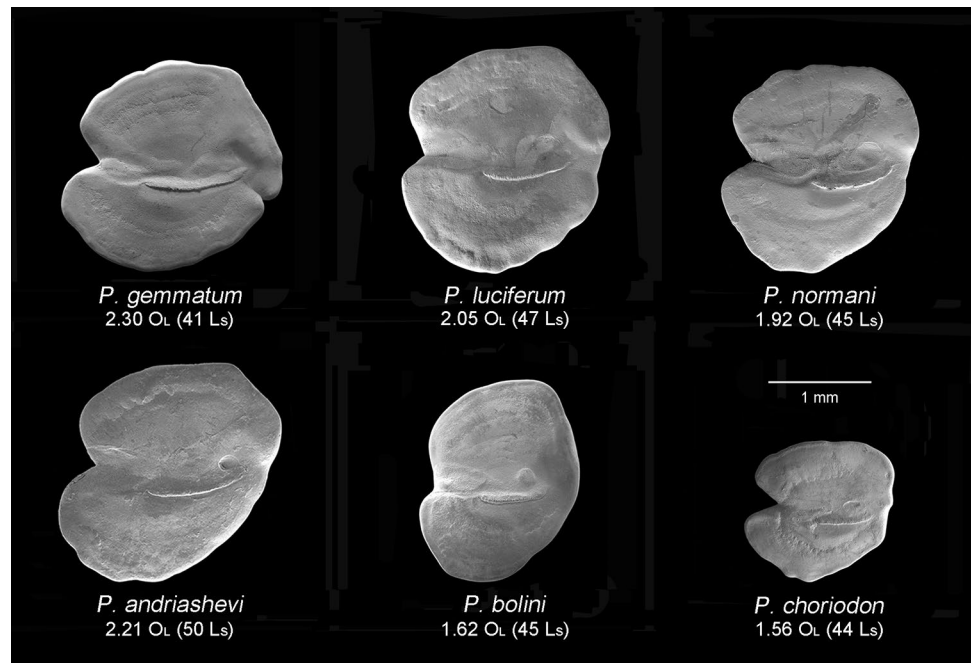


Fig. 6 Scanning electron microscopy images of the mesial (generally **a–d**) and lateral (last image) surface of selected otoliths (sagittae) of *Protomyctophum andriashevi*, *P. bolini*, *P. choriodon*, *P. gemmatum*, *P. luciferum*, *P. normani*, *P. parallelum*, and *P. tenisoni*. O_L, otolith

length in mm, L_S, fish standard length in mm. *, L_S estimated based on L_S:O_L regressions (*Protomyctophum choriodon*, Appendix; *Protomyctophum tenisoni* Reid 1996). *P. tenisoni* otolith image **d** has been flipped horizontally. Scale bar represents 1 mm

Fig. 7 Scanning electron microscopy images of the mesial surface of six similar-sized (41–50 L_S) *Protomyctophum* species showing variation in relative size and shape. O_L , otolith length in mm, L_S , fish standard length in mm. Scale bar represents 1 mm



useful taxonomic characters and can be identified to species. However, care should be taken with smaller and/or eroded otoliths as they often lack key features and can be difficult to identify.

Four myctophid species that may be found in the SO have not been included in this guide. Three species—*Ceratoscopelus warmingii*, *Lampanyctus ater*, and *Notoscopelus resplendens* — are likely rare in this region (Gon and Heemstra 1990). *Ceratoscopelus warmingii* and *N. resplendens* have broadly subtropical-tropical or tropical distributions (Hulley 1981) and likely comprise species complexes (Gaither et al. 2016; dos Santos et al. 2024), while *L. ater* has a subtropical distribution and all have only been found in Commission for the Conservation of Antarctic Marine Living Resources (CCAMLR) waters on single occasions (Gon and Heemstra 1990). *Taaningichthys bathyphilus* was also not included as it is bathypelagic (mostly captured below 1000 m depths, Hulley 1981) and therefore not available to many predators. However, this species is widespread and has been captured south of the Antarctic Polar Front (McGinnis 1982). SEM otolith images and otoliths descriptions are provided for these four taxa in Smale et al. (1995).

The identification of *Protomyctophum* species (and their otoliths) proved difficult. Species in this genus are fragile and easily damaged during capture, and their otoliths are difficult to distinguish. This study utilised DNA barcoding to assist with the identification of two problematic species: *P. gemmatum* and *P. luciferum*. Large males were often readily identifiable by key characters, such as the number of pelvic rays (15 or less in *P. luciferum* versus 16 or more in *P. gemmatum*, *vide* Hulley 1981) and the relative size

of the supracaudal and infracaudal glands (Hulley 1981). However, identifying small specimens and females was often problematic. Some specimens differed from published diagnostic criteria from Hulley (1981). For example, two specimens genetically identified as *P. luciferum* had unusual morphological features. One specimen had 16 pectoral rays, while the other had supracaudal and infracaudal glands of the same size. Therefore, we recommend caution when identifying *Protomyctophum* specimens, in particular *P. gemmatum* and *P. luciferum*.

Based on otolith size, *S. boops* may comprise two species: *S. boops* and a second taxa with relatively smaller otoliths (based on four specimens), which could represent *Symbolophorus* sp. C (McGinnis 1982). *Symbolophorus* sp. C was mentioned by Waite (1911) (as '*Myctophum humboldti*') and McGinnis (1982); this species is only known from the East Coast of Aotearoa New Zealand (McGinnis 1982). Both *Symbolophorus* taxa were included in an inhouse NIWA myctophid guide and separated mainly by eye diameter (10–12% L_S in *Symbolophorus* sp. C and 8–9% L_S in *S. boops* [as *Symbolophorus* sp. B]). However, Roberts et al. (2015) only recognised a single species (*S. boops*) and mentioned there 'appears to be ontogenetic variation in eye size in this species' (p. 678).

Previous studies have also revealed two potentially new species of *Gymnoscopelus* (Smith et al. 2012; McBride et al. 2022), and there were two types of *Gymnoscopelus piabilis* otoliths in this study. Genetic and taxonomic research is needed to resolve these uncertainties.

The otolith descriptions in the present study were limited by sample availability. Some species, such as *Hintonia candens*, *Lampadena speculigera*, *Lampanyctus lepidolichnus*, *Metelectrona herwigi*, *Protomyctophum parallelum*, and *P. tenisoni*, were only represented by a few (1–10) otoliths. Other species, such as *Gymnoscopelus nicholsi* and *G. piabilis* A were only represented by otoliths from large individuals. Although, we may not have adequately captured ontogenetic or intraspecific variability in the otoliths of these species, our study provides diagnostic characters that can be used to identify the otoliths of 37 SO myctophid species. Future studies should focus on including a range of specimens of different sizes and from a wide geographic range in order to describe ontogenetic and intraspecific variability. Furthermore, extending these studies to other SO mesopelagic fish taxa would greatly improve prey identification in diet studies. Otoliths from small specimens (< *c.* 30 mm L_S) of several SO myctophid species (and other SO mesopelagic species) were illustrated by Williams and McEldowney (1990), which is a useful reference.

The otoliths of most SO myctophid species were relatively uniform with logical ontogenetic development. However, otoliths from larger individuals of several species showed unexpected differences: *G. opisthopterus* (varied in the degree of rostral development), *G. piabilis* (in otolith length and the size of the excisura), *Lampanyctus intricarius* (in the relative size of the rostra), and *L. macdonaldi* (in otolith length). This may be related to variability in somatic and otolith growth rates in larger longer-lived species (myctophid life cycles last between 2 and 7 years; Saunders et al. 2019, 1987), or, in the case of *G. piabilis*, our samples may include two species (McBride et al. 2022).

In alignment with previous myctophid otolith studies (e.g., Schwarzhans 1981 (1984), 2013, 2019; Hecht 1987; Williams and McEldowney 1990; Reid 1996; Smale et al. 1995), this study focused on the mesial (inner) surface of the otolith, which is the most useful diagnostically. However, we also captured an SEM image of the lateral (outer) surface of a representative otolith of each species (Figs. 2, 3, 4, 5 and 6). On the lateral otolith surface of some species, several ridges radiate out (radial ribs; Schwarzhans 1981 (1984)) from the nuclear region reflecting underlying epitaxial growth (e.g., *D. ostenfeldi* or *G. bolini*, Figs. 2, 4). These ridges are generally more pronounced ventrally and may extend to form sculpturing at the margin (e.g., the serrate ventral margins of *D. ostenfeldi*, *G. bolini*, and *L. notialis*). Similarly on some species, the ostial furrow may be visible on the lateral surface (e.g., *G. bolini* or *G. piabilis* B (Fig. 4)). Radial ridges and the ostial furrow may be useful diagnostically,

particularly if the otolith margin is eroded. Future studies should consider including the lateral surface in otolith descriptions. The curvature of the mesial and lateral faces of the otolith are also useful diagnostically (Schwarzhans 2013), but this feature can be difficult to capture and was not used in the current study.

We have also included O_L to L_S regressions and M_T to L_S regressions for 32 SO myctophid species (Appendix). These data complement those provided in earlier studies (e.g., Adams and Klages 1987; Hecht 1987; Williams and McEldowney 1990; Smale et al. 1995; Reid 1996; Cheral et al. 1997; Furlani et al. 2007; Saunders et al. 2021). They can enable fish size, mass, and energetic content to be estimated (Saunders et al. 2021) in dietary investigations based on stomach content analysis (e.g., fishes, squids, birds) and scat analysis (e.g., pinnipeds). Carbon export models also require species-specific traits, such as fish mass, to estimate metabolic rates and more accurately quantify the contribution of mesopelagic fishes to active carbon fluxes (e.g., Woodstock et al. 2022). These models heavily rely on estimates of mesopelagic fish biomass, which are often obtained using fisheries acoustics. Otolith length-to-fish standard length regressions and fish mass can be used to reconstruct the size structure of mesopelagic fish communities in data-deficient areas. The ratio of fish length to weight are critical inputs for converting fisheries acoustic density estimates into fish biomass (e.g., Irigoien et al. 2014; Escobar-Flores et al. 2020).

This study provided brief descriptions and SEM otolith (sagitta) images for 37 species of SO myctophids and allometric equations for 32 of these species. The otoliths of most SO myctophids were distinctive and able to be identified to genus and often species level and are a powerful tool for identifying myctophid prey in trophic studies. However, for some species, our sample sizes were small or restricted to otoliths from large fish. Future studies of SO myctophid otoliths should include a comprehensive size range of otoliths for all species. Furthermore, otoliths recovered from the stomachs of predators or archaeological deposits may be eroded and lack key diagnostic criteria. Images of partially eroded otoliths alongside intact otoliths would greatly facilitate otolith identification.

Appendix

See Tables 1 and 2.

Table 1 Number of fish examined and fish standard length (L_S , mm): otolith (sagitta) length (O_L , mm) regression parameters (where sufficient samples were available) for 37 Southern Ocean myctophid species

Species	n	a	b	r^2	L_S range (mm)	O_L range (mm)	$O_L@50L_S$ (mm)
<i>Diaphus danae</i>	88	10.214	1.3663	0.97	37–115	2.44–6.04	3.20
<i>D. hudsoni</i>	65	17.806	0.9725	0.97	30–79	1.81–4.79	3.13
<i>D. ostenfeldi</i>	65	14.008	1.2408	0.98	33–129	2.09–5.97	2.79
<i>Electrona antarctica</i>	77	39.293	0.9963	0.99	26–103	0.65–2.57	1.27
<i>E. carlsbergi</i>	65	21.735	1.0191	0.94	56–101	2.57–4.52	2.25
<i>E. paucirastra</i> *(4)	60	20.167	1.0538	0.95	23–73	1.13–3.35	2.37
<i>E. subaspera</i> *(1)	33	21.185	1.1257	0.96	24–114	1.00–4.28	2.13
<i>Gymnoscopelus bolini</i> *(6)	41	20.007	1.1452	0.98	31–255	1.50–9.52	2.22
<i>G. braueri</i>	72	42.207	0.9904	0.98	36–126	0.85–2.91	1.18
<i>G. fraseri</i>	29	21.399	1.0109	0.87	54–89	2.48–4.18	2.30
<i>G. hintonoides</i>	29	14.124	1.4262	0.93	55–146	2.64–5.06	2.42
<i>G. microlampas</i>	18	19.552	1.2065	0.84	81–126	3.25–4.71	2.17
<i>G. nicholsi</i> *(1)	54	28.823	0.9266	0.84	31–168	1.07–6.60	1.81
<i>G. opisthopterus</i>	55	58.961	0.9575	0.89	67–170	1.18–3.48	0.84
<i>G. piabilis</i>	58	20.023	1.0392	0.97	34–132	1.83–6.26	2.41
<i>Hintonia candens</i>	2	–	–	–	76–90	3.62–3.86	–
<i>Krefflichthys anderssoni</i>	71	32.477	1.3283	0.97	15–67	0.52–1.80	1.38
<i>Lampadena notialis</i>	23	15.987	1.032	0.97	49–159	3.16–9.27	3.02
<i>L. speculigera</i>	8	14.6	1.1925	0.90	45–140	2.63–7.23	2.79
<i>Lampanyctodes hectoris</i>	57	18.084	1.4334	0.91	23–63	1.13–2.71	2.03
<i>Lampanyctus achirus</i>	44	103.73	1.1725	0.71	64–164	0.76–1.60	0.54
<i>L. australis</i>	90	36.824	1.0243	0.94	27–113	0.85–3.05	1.34
<i>L. intricarius</i>	91	36.659	1.3135	0.76	77–212	1.85–3.89	1.26
<i>L. lepidolichnus</i>	3	–	–	–	83–117	1.62–1.93	–
<i>L. macdonaldi</i>	36	82.195	0.4681	0.35	77–127	1.28–2.59	0.34
<i>Lampichthys procerus</i>	60	20.898	1.1056	0.98	35–95	1.51–4.09	2.20
<i>Metellectrona herwigii</i>	3	–	–	–	31–50	1.43–2.43	–
<i>M. ventralis</i>	54	22.69	0.9215	0.90	42–88	2.18–4.5	2.35
<i>Protomyctophum andriashevi</i>	16	21.007	1.1066	0.94	33–57	1.43–2.36	2.17
<i>P. bolini</i> (outer Ross Sea)	33	19.884	1.4481	0.91	25–53	1.15–2.01	1.89
<i>P. bolini</i> (NZ sub-Antarctic)	61	24.091	1.0213	0.70	34–55	1.41–2.08	2.03
<i>P. choriodon</i>	21	22.588	1.475	0.98	35–91	1.33–2.56	1.71
<i>P. gemmatum</i>	17	13.213	1.3186	0.97	29–80	1.89–3.90	2.74
<i>P. luciferum</i>	111	24.364	0.8745	0.88	42–70	1.91–3.32	2.27
<i>P. normani</i>	97	14.416	1.7453	0.90	27–57	1.44–2.26	2.03
<i>P. parallelum</i>	1	–	–	–	37	1.70	–
<i>P. tenisoni</i>	6	–	–	–	30–43 [#]	1.11–1.37	–
<i>Symbolophorus boops</i>	63	24.721	0.8999	0.95	58–146	2.69–6.97	2.18

$L_S = a O_L^b$. $O_L@50L_S$, the estimated O_L at 50 mm L_S based on regression data. n , total number of specimens examined; a and b are the regression constants; r^2 , coefficient of determination. *(), data supplemented by small fish from Williams and McEldowney (1990), number of fish in brackets; [#], L_S estimated based on $L_S:O_L$ regression from Reid (1996). *Gymnoscopelus piabilis* data includes type A and B otoliths.

Table 2 Number of fish examined and fish standard length (L_S , mm): fish total mass (M_T , g) regression parameters (where sufficient samples were available) for 37 Southern Ocean myctophid species

Species	n	a	b	r^2	L_S range (mm)	M_T range (g)	$M_T@50L_S$ (g)
<i>Diaphus danae</i>	93	40.7	0.3254	0.98	37–115	0.8–30.8	1.88
<i>D. hudsoni</i>	68	41.192	0.2867	0.99	30–79	0.4–8.2	1.96
<i>D. ostenfeldi</i>	65	40.89	0.2985	0.98	33–129	0.6–39.6	1.96
<i>Electrona antarctica</i>	80	46.363	0.2809	0.99	26–103	0.1–16.7	1.31
<i>E. carlsbergi</i>	60	43.951	0.2806	0.94	56–101	3.0–21.1	1.58
<i>E. paucirastra</i>	58	40.373	0.3117	0.98	23–73	0.2–5.8	1.99
<i>E. subaspera</i>	30	41.883	0.3009	0.99	44–114	1.2–30.5	1.80
<i>Gymnoscopelus bolini</i>	37	45.337	0.3286	0.99	61–255	2.4–200.3	1.35
<i>G. braueri</i>	73	53.999	0.2821	0.99	36–126	0.2–20.5	0.76
<i>G. fraseri</i>	31	49.261	0.2724	0.93	54–89	1.4–9.2	1.06
<i>G. hintonoides</i>	29	48.05	0.292	0.96	55–146	1.5–35.2	1.15
<i>G. microlampas</i>	13	50.381	0.2938	0.98	85–126	5.9–23.6	0.98
<i>G. nicholsi</i>	64	52.54	0.2849	0.76	123–168	21.0–58.6	0.84
<i>G. opisthopterus</i>	57	54.885	0.2868	0.99	67–170	2.0–52.3	0.72
<i>G. piabilis</i>	57	47.452	0.3197	1.00	34–132	0.4–22.6	1.18
<i>Hintonia candens</i>	2	–	–	–	76–90	8.5–13.4	–
<i>Krefflichthys anderssoni</i>	73	46.545	0.2926	0.98	15–67	0.0–3.1	1.28
<i>Lampadena notialis</i>	25	42.48	0.3069	0.99	49–159	1.5–73.8	1.70
<i>L. speculigera</i>	10	40.535	0.3217	0.94	45–141	1.4–48.3	1.92
<i>Lampanyctodes hectoris</i>	59	42.971	0.3086	0.98	23–63	0.1–3.7	1.64
<i>Lampanyctus achirus</i>	44	64.205	0.2547	0.94	64–164	0.9–34	0.37
<i>L. australis</i>	85	48.007	0.3127	0.98	27–113	0.2–14.1	1.14
<i>L. intricarius</i>	95	55.104	0.3028	0.95	77–212	2.9–74.8	0.73
<i>L. lepidolichnus</i>	3	–	–	–	83–117	5.1–19.4	–
<i>L. macdonaldi</i>	38	59.657	0.2574	0.82	77–127	3.1–20.9	0.49
<i>Lampichthys procerus</i>	65	46.543	0.3092	0.99	35–95	0.4–9.8	1.26
<i>Metellectrona herwigii</i>	3	–	–	–	31–50	0.4–2.1	–
<i>M. ventralis</i>	57	39.395	0.3128	0.97	42–88	1.1–12.6	2.14
<i>Protomyctophum andriashevi</i>	14	40.502	0.3223	0.89	36–53	0.7–2.2	1.92
<i>P. bolini</i> (outer Ross Sea)	33	43.434	0.2766	0.96	25–53	0.1–2.1	1.66
<i>P. bolini</i> (NZ sub-Antarctic)	60	42.235	0.3021	0.93	34–55	0.5–2.2	1.75
<i>P. choriodon</i>	23	43.463	0.3243	0.99	35–91	0.4–9.5	1.54
<i>P. gemmatum</i>	23	40.188	0.325	0.99	29–80	0.4–7.7	1.96
<i>P. luciferum</i>	125	42.527	0.2772	0.92	42–70	1.1–5.5	1.79
<i>P. normani</i>	99	39.959	0.3101	0.96	27–57	0.3–2.8	2.06
<i>P. parallelum</i>	1	–	–	–	37	0.3	–
<i>P. tenisoni</i>	6	–	–	–	30–43 [#]	–	–
<i>Symbolophorus boops</i>	63	42.747	0.3262	0.97	58–146	2.5–53.3	1.61

$L_S = a M_T^b$. $M_T@50L_S$, the M_T at 50 mm L_S based on regression data. n , total number of specimens examined; a and b are the regression constants; r^2 , coefficient of determination. [#], L_S estimated based on $L_S:O_L$, regression from Reid (1996). *Gymnoscopelus piabilis* data includes type A and B otoliths.

Acknowledgements We thank Raoul Solomon (formerly Massey University) who prepared otoliths and captured SEM micrographs in this study. Paul Grimes (deceased, formerly NIWA), Peter McMullan (Museum of New Zealand Te Papa Tongarewa), and P. Alexander (Butch) Hulley (Iziko Museums of Cape Town, South Africa) provided taxonomic advice and helped identify myctophids, and Jeff Forman (NIWA) collected and identified specimens. Stuart Hanchet (retired, formerly NIWA) and Chris Jones (NOAA Fisheries, USA) provided otoliths from off the South Shetland Islands. Erika MacKay (formerly NIWA) and Peter Marriott (NIWA) provided advice on Adobe® Photoshop®. We thank Jeff Forman, Werner Schwarzhans (University of Copenhagen), and an anonymous reviewer for their helpful and constructive feedback on the draft manuscript.

Author contributions D.S. and Y.C. conceived and designed the research, and contributed otoliths. L.M. prepared otoliths for scanning electron microscopy (SEM) and provided logistical support with Massey University. D.H. and Y.H. prepared otoliths and captured SEM micrographs. D.S. edited the SEM otolith images and prepared the figures. H.B. barcoded tissue samples. D.S., Y.C., H.B., and P.E.F. drafted the manuscript, and M.P. provided funding for the study. The manuscript has been edited, read, and approved by D.S., H.B., L.M., P.E.F., M.P., Y.H., and Y.C.

Funding The project was co-funded by the New Zealand Ministry for Business, Innovation and Employment (MBIE) through Ross-RAMP (C01X1710), SSIF (NIWA Oceans Centre “Structure and function of marine ecosystems”), New Zealand Antarctic Science Platform (Project 3, ANTA1801), and NIWA structured internal projects (SIPs). Yves Chérel was funded by the Centre National de la Recherche Scientifique (CNRS), and, in the field, by the Institut Polaire Français Paul Emile Victor (IPEV, Programme No. 109, C. Barbraud). DNA barcoding was funded by the Auckland University of Technology.

Data availability The data that support the regression parameters can be made available by the corresponding author upon reasonable request. DNA sequences were uploaded to the Barcode of Life Data System public project titled ‘Lanternfish from Aotearoa’ (project code: LAN) and then submitted to GenBank with sample codes PQ351974–PQ352001.

Code availability Not applicable.

Declarations

Conflict of interest The authors declare no competing interests.

Ethical approval Most fish used in this research were collected by fine meshed mesopelagic and demersal research trawls under special permit for the New Zealand Ministry for Primary Industries. This project only worked on dead animals, so there were no specific ethical considerations. Kerguelen Fieldwork was approved by the Conseil des Programmes Scientifiques et Technologies Polaires of the Institut Polaire Français Paul Emile Victor (IPEV), and procedures were approved by the Animal Ethics Committee of IPEV. No fish were CITES listed.

Open Access This article is licensed under a Creative Commons Attribution-NonCommercial-NoDerivatives 4.0 International License, which permits any non-commercial use, sharing, distribution and reproduction in any medium or format, as long as you give appropriate credit to the original author(s) and the source, provide a link to the Creative Commons licence, and indicate if you modified the licensed material. You do not have permission under this licence to share adapted material derived from this article or parts of it. The images or other third party material in this article are included in the article’s Creative Commons

licence, unless indicated otherwise in a credit line to the material. If material is not included in the article’s Creative Commons licence and your intended use is not permitted by statutory regulation or exceeds the permitted use, you will need to obtain permission directly from the copyright holder. To view a copy of this licence, visit <http://creativecommons.org/licenses/by-nc-nd/4.0/>.

References

- Adams NJ, Klages NT (1987) Seasonal variation in the diet of king penguins (*Aptenodytes patagonicus*) at sub-Antarctic Marion Island. *J Zool* 212:303–324. <https://doi.org/10.1111/j.1469-7998.1987.tb05992.x>
- Braid HE, McBride PD, Bolstad KSR (2014) Molecular phylogenetic analysis of the squid family Mastigoteuthidae (Mollusca, Cephalopoda) based on three mitochondrial genes. *Hydrobiologia* 725:145–164. <https://doi.org/10.1007/s10750-013-1775-3>
- Brown CR, Klages NT (1987) Seasonal and annual variation in diets of Macaroni (*Eudyptes chrysolophus chrysolophus*) and Southern rockhopper (*E. chrysocome chrysocome*) penguins at sub-Antarctic Marion Island. *J Zool* 212:7–28. <https://doi.org/10.1111/j.1469-7998.1987.tb05111.x>
- Chérel Y, Guinet C, Tremblay Y (1997) Fish prey of Antarctic fur seals *Arctocephalus gazella* at Ile de Croix, Kerguelen. *Polar Biol* 17:87–90. <https://doi.org/10.1007/s003000050109>
- Chérel Y, Pütz K, Hobson KA (2002) Summer diet of king penguins (*Aptenodytes patagonicus*) at the Falkland Islands, southern Atlantic Ocean. *Polar Biol* 25:898–906. <https://doi.org/10.1007/s00300-002-0419-2>
- Chérel Y, Fontaine C, Richard P, Labat J-P (2010) Isotopic niches and trophic levels of myctophid fishes and their predators in the Southern Ocean. *Limnol Oceanogr* 55:324–332. <https://doi.org/10.4319/lo.2010.55.1.0324>
- Collins MA, Ross KA, Belchier M, Reid K (2007) Distribution and diet of juvenile Patagonian toothfish on the South Georgia and Shag Rocks shelves (Southern Ocean). *Mar Biol* 152:135–147. <https://doi.org/10.1007/s00227-007-0667-3>
- Connan M, Chérel Y, Mayzaud P (2007) Lipids from stomach oil of procellariiform seabirds document the importance of myctophid fish in the Southern Ocean. *Limnol Oceanogr* 52:2445–2455. <https://doi.org/10.4319/lo.2007.52.6.2445>
- Davison PC, Checkley DM Jr, Koslow JA, Barlow J (2013) Carbon export mediated by mesopelagic fishes in the northeast Pacific Ocean. *Prog Oceanogr* 116:14–30. <https://doi.org/10.1016/j.pocean.2013.05.013>
- Dornan T, Fielding S, Saunders RA, Genner MJ (2022) Large mesopelagic fish biomass in the Southern Ocean resolved by acoustic properties. *Proc R Soc B Biol Sci* 289:20211781. <https://doi.org/10.1098/rspb.2021.1781>
- dos Santos LF, Pontes AI, Nunes DBSM, Farias MCL, dos Santos DM, Jacobina UP (2024) Seven species in one? DNA barcoding reveals high cryptic diversity in *Ceratoscopelus warmingii* (Myctophiformes, Myctophidae) a circumglobal mesopelagic species. *Thalassas* 40:1031–1040. <https://doi.org/10.1007/s41208-024-00689-z>
- Duhamel G, Gasco N, Davaine P (2005) Poissons des îles Kerguelen et Crozet: guide régional de l’océan Austral. Collection Patrimoines Naturels, 63. Muséum national d’Histoire naturelle: Paris. 419 pp.
- Escobar-Flores PC, O’Driscoll RL, Montgomery JC, Ladroit Y, Jendersie S (2020) Estimates of density of mesopelagic fish in the Southern Ocean derived from bulk acoustic data collected by ships of opportunity. *Polar Biol* 43:43–61. <https://doi.org/10.1007/s00300-019-02611-3>

- Folmer O, Black M, Hoeh W, Lutz R, Vrijenhoek R (1994) DNA primers for amplification of mitochondrial cytochrome c oxidase subunit I from diverse metazoan invertebrates. *Mol Mar Biol Biotechnol* 3:294–299
- Fricke R, Eschmeyer WN, Van der Laan R (eds) (2024) Eschmeyer's Catalog of Fishes: Genera, Species, References. (<http://researcharchive.calacademy.org/research/ichthyology/catalog/fishcatmain.asp>). Electronic version accessed 20 Sep 2024.
- Furlani D, Gales R, Pemberton D (2007) Otoliths of common Australian temperate fish: a photographic guide. CSIRO Publishing, Clayton, 208 p.
- Gaither MR, Bowen BW, Rocha LA, Briggs JC (2015) Fishes that rule the world: circumtropical distributions revisited. *Fish Fish* 17:664–679. <https://doi.org/10.1111/faf.12136>
- Goldsworthy SD, He X, Tuck GN, Lewis M, Williams R (2001) Trophic interactions between the Patagonian toothfish, its fishery, and seals and seabirds around Macquarie Island. *Mar Ecol Prog Ser* 218:283–302. <https://doi.org/10.3354/meps218283>
- Gon O, Heemstra PC (eds) (1990) Fishes of the Southern Ocean. J.L.B. Smith Institute of Ichthyology, Grahamstown, 462 p.
- Hecht T (1987) A guide to the Otoliths of Southern Ocean fishes. *S Afr J Antarct Res* 71:1–87
- Hulley PA (1981) Results of the research cruises of FRV "Walter Herwig" to South America. LVIII. Family Myctophidae (Osteichthyes, Myctophiformes). *Arch Fischereiwiss* 31. 300 p.
- Irigoin X, Klevjer TA, Røstad A, Martinez U, Boyra G, Acuña JL, Bode A, Echevarria F, Gonzalez-Gordillo JI, Hernandez-Leon S, Agusti S, Aksnes DL, Duarte CM, Kaartvedt S (2014) Large mesopelagic fishes biomass and trophic efficiency in the open ocean. *Nat Commun* 5:3271. <https://doi.org/10.1038/ncomms4271>
- Ivanova NV, Zemlak TS, Hanner RH, Hebert PDN (2007) Universal primer cocktails for fish DNA barcoding. *Mol Ecol Notes* 7:544–548. <https://doi.org/10.1111/j.1471-8286.2007.01748.x>
- Koken E (1884) Über Fisch-Otolithen, insbesondere über diejenigen der norddeutschen Oligozän-Ablagerungen. *Z Dtsch Geol Ges* 36:500–565
- Lancraft TM, Torres JJ, Hopkins TL (1989) Micronekton and macrozooplankton in the open waters near Antarctic ice edge zones (AMERIEZ 1983 and 1986). *Polar Biol* 9:225–233. <https://doi.org/10.1007/BF00263770>
- Martin RP, Olson EE, Girard MG, Smith WL, Davis MP (2018) Light in the darkness: new perspective on lanternfish relationships and classification using genomic and morphological data. *Mol Phylogenet Evol* 121:71–85. <https://doi.org/10.1016/j.ympev.2017.12.029>
- McBride LE, Braid HE, Stevens DW, Bolstad KSR (2022) Trophic ecology of the deep-sea squid *Moroteuthopsis ingens* (Cephalopoda: Onychoteuthidae) from the Chatham Rise, Aotearoa New Zealand. *NZ J Mar Freshw* 57:582–596. <https://doi.org/10.1080/00288330.2022.2086268>
- McGinnis RF (1982) Biogeography of Lanternfishes (Myctophidae) South of 30°S. *Ant Res Ser* 35. 110 p. <https://doi.org/10.1029/AR035>
- Phillips KL, Jackson GD, Nichols PD (2001) Predation on myctophids by the squid *Moroteuthis ingens* around Macquarie and Heard Islands: stomach contents and fatty acid analyses. *Mar Ecol Prog Ser* 215:179–189. <https://doi.org/10.3354/meps215179>
- Ratnasingham S, Hebert PD (2007) BOLD: the barcode of life data system (<http://www.barcodinglife.org>). *Mol Ecol Notes* 7:355–364. <https://doi.org/10.1111/j.1471-8286.2007.01678.x>
- Ratnasingham S, Hebert PDN (2013) A DNA-based registry for all animal species: the barcode index number (BIN) system. *PLoS One* 8:e66213. <https://doi.org/10.1371/journal.pone.0066213>
- Reid K (1996) A guide to the use of otoliths in the study of predators at South Georgia. British Antarctic Survey. Cambridge, UK, 40 p.
- Reisinger RR, Landman M, Mgibantakaa N, Smale MJ, Bester MN, De Bruyn PJN, Pistorius PA (2018) Overlap and temporal variation in the diets of sympatric Antarctic and Subantarctic fur seals (*Arctocephalus* spp.) at Marion Island, Prince Edward Islands. *Polar Res* 37:1451142. <https://doi.org/10.1080/17518369.2018.1451142>
- Roberts CD, Stewart AL, Struthers CD (eds) (2015) The fishes of New Zealand. In: 4 volumes. Te Papa Press, Wellington, New Zealand, 2008 p.
- Rodhouse PG, White MG, Jones MRR (1992) Trophic relations of the cephalopod *Martialia hyadesi* (Teuthoidea: Ommastrephidae) at the Antarctic Polar Front, Scotia Sea. *Mar Biol* 114:415–421. <https://doi.org/10.1007/BF00350032>
- Sabourenkov E (1992) Myctophids in the diet of Antarctic predators. *Comm Conserv Antarct Mar Liv Res Sel Sci Papers* 1991: 335–368. Retrieved from https://www.ccamlr.org/en/system/files/science_journal_papers/21-Sabourenkov.pdf
- Saunders RA, Hill SL, Tarling GA, Murphy EJ (2019) Myctophid fish (Family Myctophidae) are central consumers in the food web of the Scotia Sea (Southern Ocean). *Front Mar Sci* 6:530. <https://doi.org/10.3389/fmars.2019.00530>
- Saunders RA, Lourenço S, Vieira RP, Collins MA, Xavier JC (2021) Length–weight and otolith size to standard length relationships in 12 species of Southern Ocean Myctophidae: A tool for predator diet studies. *J Appl Ichthyol* 37:140–144. <https://doi.org/10.1111/jai.14126>
- Schwarzahns W (1984) Fish otoliths from the New Zealand tertiary. A translation of 'Die tertiäre Teleosteer-Fauna Neuseelands, rekonstruiert anhand von Otolithen' (1981). *Berliner Geowissenschaftliche Abhandlungen, Reihe A: Geologie und Paleontologie* 26. 211 p. *N Z Geol Surv* 113. 269 p.
- Schwarzahns W (2013) A comparative morphological study of the recent otoliths of the genera *Diaphus*, *Idiolychnus* and *Lobianchia* (Myctophidae). *Palaeo Ichthyol* 13:41–82. <https://doi.org/10.13140/2.1.2872.3843>
- Schwarzahns W (2019) Reconstruction of the fossil marine bony fish fauna (Teleostei) from the Eocene to Pleistocene of New Zealand by means of otoliths. *Mem Soc ital sci nat Mus civ stor nat Milano* 46:1–326
- Smale MJ, Watson G, Hecht T (1995) Otolith atlas of southern African marine fishes. *Ichthyological Monographs of the J.L.B. Smith Inst Ichthyol* 1(14):253
- Smith MM, Heemstra PC (eds) (2003) Smiths' sea fishes. Struik Publishers, Johannesburg, p 1047
- Smith PJ, Steinke D, Dettai A, McMillan P, Welsford D, Stewart A, Ward RD (2012) DNA barcodes and species identifications in Ross Sea and Southern Ocean fishes. *Polar Biol* 35:1297–1310. <https://doi.org/10.1007/s00300-012-1173-8>
- Waite ER (1911) Pisces, Part II. *Rec Canterbury Mus* 1(3):157–272. Retrieved from <https://www.biodiversitylibrary.org/item/93234>
- Williams R, McEldowney A (1990) A guide to the fish otoliths from waters off the Australian Antarctic territory, Heard and Macquarie Islands. *Anare Research Notes* 75. Antarctic Division, Australia, 173 p.
- Woodstock MS, Sutton TT, Zhang Y (2022) Corrigendum: a trait-based carbon export model for mesopelagic fishes in the Gulf of Mexico with consideration of asynchronous vertical migration, flux boundaries, and feeding guilds. *Limnol Oceanogr* 67:2117–2117. <https://doi.org/10.1002/lno.12176>

Publisher's Note Springer Nature remains neutral with regard to jurisdictional claims in published maps and institutional affiliations.